



Contents lists available at ScienceDirect

Science of the Total Environment

journal homepage: www.elsevier.com/locate/scitotenv

Methylmercury production in sediment from agricultural and non-agricultural wetlands in the Yolo Bypass, California, USA

Mark Marvin-DiPasquale^{a,*}, Lisamarie Windham-Myers^a, Jennifer L. Agee^a, Evangelos Kakouros^a, Le H. Kieu^a, Jacob A. Fleck^b, Charles N. Alpers^b, Craig A. Stricker^c

^a U.S. Geological Survey, 345 Middlefield Road, Mailstop 480, Menlo Park, CA 94025, USA

^b U.S. Geological Survey, Placer Hall, 6000 J St., Sacramento, CA 95819, USA

^c U.S. Geological Survey, Fort Collins Science Center, Building 21, Mailstop 963, Denver, CO 80225, USA

HIGHLIGHTS

- Hg biogeochemistry was compared for agricultural and non-agricultural wetland soils.
- MeHg concentrations were higher in agricultural wetland soils.
- Hg(II) availability for microbial methylation was linked to wetland management.
- Fe and S chemistry drove temporal changes in Hg cycling.

ARTICLE INFO

Article history:

Received 6 August 2012

Received in revised form 27 September 2013

Accepted 28 September 2013

Available online xxxx

Editor: Mae Sexauer Gustin

Keywords:

Methylmercury production

Sediment

Wetlands

Rice agriculture

Iron-reduction

Sulfate-reduction

ABSTRACT

As part of a larger study of mercury (Hg) biogeochemistry and bioaccumulation in agricultural (rice growing) and non-agricultural wetlands in California's Central Valley, USA, seasonal and spatial controls on methylmercury (MeHg) production were examined in surface sediment. Three types of shallowly-flooded agricultural wetlands (white rice, wild rice, and fallow fields) and two types of managed (non-agricultural) wetlands (permanently and seasonally flooded) were sampled monthly-to-seasonally. Dynamic seasonal changes in readily reducible 'reactive' mercury (Hg(II)_R), Hg(II)-methylation rate constants (k_{meth}), and concentrations of electron acceptors (sulfate and ferric iron) and donors (acetate), were all observed in response to field management hydrology, whereas seasonal changes in these parameters were more muted in non-agricultural managed wetlands. Agricultural wetlands exhibited higher sediment MeHg concentrations than did non-agricultural wetlands, particularly during the fall through late-winter (post-harvest) period. Both sulfate- and iron-reducing bacteria have been implicated in MeHg production, and both were demonstrably active in all wetlands studied. Stoichiometric calculations suggest that iron-reducing bacteria dominated carbon flow in agricultural wetlands during the growing season. Sulfate-reducing bacteria were not stimulated by the addition of sulfate-based fertilizer to agricultural wetlands during the growing season, suggesting that labile organic matter, rather than sulfate, limited their activity in these wetlands. Along the continuum of sediment geochemical conditions observed, values of k_{meth} increased approximately 10,000-fold, whereas Hg(II)_R decreased 100-fold. This suggests that, with respect to the often opposing trends of Hg(II)-methylating microbial activity and Hg(II) availability for methylation, microbial activity dominated the Hg(II)-methylation process, and that along this biogeochemical continuum, conditions that favored microbial sulfate reduction resulted in the highest calculated MeHg production potential rates. Rice straw management options aimed at limiting labile carbon supplies to surface sediment during the post-harvest fall-winter period may be effective in limiting MeHg production within agricultural wetlands.

Published by Elsevier B.V.

1. Introduction

The bioaccumulation of toxic methylmercury (MeHg) in aquatic food webs is of concern for wildlife and human health. From wet meadows and lowland forests (Bradley et al., 2011), to hardwood swamps (Hall et al., 2008), peatlands (Mitchell et al., 2009), floodplains (Roulet et al., 2001), freshwater marshes (Gilmour et al., 1998) and saltmarshes (Marvin-DiPasquale et al., 2003a), wetlands are known to

* Corresponding author. Tel.: +1 650 329 4442; fax: +1 650 329 4463.

E-mail addresses: mmarvin@usgs.gov (M. Marvin-DiPasquale), lwindham@usgs.gov (L. Windham-Myers), jlagee@usgs.gov (J.L. Agee), kakouros@usgs.gov (E. Kakouros), lkieu@usgs.gov (L.H. Kieu), jfleck@usgs.gov (J.A. Fleck), cnalpers@usgs.gov (C.N. Alpers), cstricker@usgs.gov (C.A. Stricker).

be significant settings for MeHg production. However, the term 'wetlands' describes an extremely diverse range of habitats that vary in terms of hydrology, salinity, climatic setting and vegetation; the common feature among them being "...constant or recurrent, shallow inundation or saturation at or near the surface of the substrate" (National Research Council, 1995). Given this broad definition and wide range of ecological settings, MeHg production efficiency likely differs among wetland settings. As the number of wetland mercury (Hg) studies increases, insight has been gained into which wetland types might be more (or less) poised for enhanced MeHg production, and the relative importance of the environmental factors that control the Hg(II)-methylation process.

Agricultural wetlands, and specifically those associated with rice cultivation, are one wetland category that has received little attention in terms of MeHg production. This lack of attention is surprising given that rice fields are estimated to cover 1.5 million km² of the earth's land-mass (Czech and Parsons, 2002). This bias may be due in part to the fact that these highly manipulated landscapes are often not considered as part of the spectrum of 'natural' wetland types that provide documented ecosystem function and that are more commonly the focus of classic ecological study. However, rice fields and similar inundated agriculture landscapes (cranberry bogs, taro, and lotus root fields) are wetlands nonetheless, as defined above. Recently, studies in Asia have reported elevated total mercury (THg) and MeHg concentrations in rice grown in Hg-contaminated areas (Horvat et al., 2003; Rothenberg and Feng, 2012; Shi et al., 2005), and that MeHg accumulates much more readily than inorganic Hg(II) in the edible rice grain (Zhang et al., 2010). Estimates of MeHg intake from rice consumption by local residents range from concentrations below a threshold of concern (Rothenberg et al., 2011) to those exceeding international guidelines (Rothenberg et al., 2012). In several cases, it was concluded that rice consumption, not fish, was the primary mode of MeHg uptake into humans (Feng et al., 2008; Meng et al., 2010).

California is the second largest rice-producing state in the USA (the first being Arkansas) (USDA, 2012), with 95% of rice growing areas (approximately 2000 km²) in the Central Valley (California Rice Commission, 2011). The Sacramento–San Joaquin Delta, within the Central Valley region, drains the Coast Ranges to the west and the Sierra Nevada to the east, both of which have multiple known areas of Hg contamination associated with historic mining activities (Alpers et al., 2005; Heim et al., 2007). Fish within the Delta region have been found to have elevated Hg concentrations, and there exists a recently approved MeHg Total Maximum Daily Load (TMDL) plan for the Central Valley/Delta region (CVRWQCB, 2011). Given the legacy of Hg contamination from mining, the elevated Hg concentrations in fish, and the juxtaposition of extensive agricultural and non-agricultural wetlands in the Central Valley, a study was conducted to examine MeHg production and bioaccumulation in this region. Recent reports from this work have indicated that the agricultural wetlands associated with this region are potential 'hot spots' for MeHg bioaccumulation in resident biota (Ackerman and Eagles-Smith, 2010; Ackerman et al., 2010). As part of this larger effort, the study described herein focused on MeHg production in sediment from adjacent agricultural and non-agricultural wetlands.

Our goal in the current study was to examine controls on MeHg production in a rice growing setting, and to compare and contrast that environment with adjacent fallow agricultural wetlands and non-agricultural wetlands. This involved the analysis of a large suite of geochemical and microbiological parameters tracked through the full management cycle associated with rice production, including the growing season, the harvest period, and the post-harvest season. The methylation of inorganic divalent mercury (Hg(II)) to MeHg is largely facilitated by a subset of sulfate-reducing bacteria (SRB) (Compeau and Bartha, 1985; Gilmour et al., 1992) and iron-reducing bacteria (FeRB) (Fleming et al., 2006; Kerin et al., 2006) in anoxic sediment. Thus, MeHg production is ultimately controlled by the presence

and activity of those Hg(II)-methylating bacteria, as limited by temperature, and the availability of electron acceptors (SO₄²⁻ and Fe(III)) and/or electron donor (labile organic matter) availability, and bioavailability of Hg(II) to these bacteria (Marvin-DiPasquale and Agee, 2003; Marvin-DiPasquale et al., 2009c). Because both FeRB and SRB can play a role in Hg(II)-methylation, and because FeRB can often outcompete SRB for commonly used organic substrates when necessary electron acceptors are available (i.e. Fe(III) and SO₄²⁻, respectively) (Acht nich et al., 1995; Lovley and Phillips, 1987a), the two key objectives of this study were to determine for adjacent agricultural and non-agricultural wetlands, a) where and when each of these microbial processes dominated carbon flow (C-flow) and MeHg production, and b) what factors underlie the spatial and temporal trends observed, with respect to MeHg production and Hg speciation. To address these objectives we calculated surface sediment MeHg production potential (MPP) rates using independently measured proxies for the activity of the Hg(II)-methylating community (via ²⁰³Hg(II) radioisotope incubation) and Hg(II) availability (i.e., the SnCl₂ reducible 'reactive' mercury (Hg(II)_R) assay), conducted a detailed examination of sediment geochemistry, and estimated C-flow through microbial iron(III) reduction (FeR) and sulfate reduction (SR) by examining net temporal changes in relevant redox species.

2. Material and methods

2.1. Study area and field sampling

Three agricultural settings (white rice, wild rice, and fallow fields) and two hydrologically distinct non-agricultural settings (seasonally flooded and permanently flooded wetlands) were sampled. The species *Oryza sativa* was grown in the 'white rice' fields, while the specialty crop *Zizania palustris* was grown in the 'wild rice' fields. Two separate fields were sampled for each of the three agricultural wetland types. One seasonally flooded wetland (SW) was sampled. Of the two permanent wetlands (PW2 and PW5), three sub-habitats were sampled in PW5: non-vegetated open-water (PW5-ow), cattail (*Typha* sp.) dominated (PW5-cat), and tule (*Scirpus* sp.) dominated (PW5-tule), all of which were within 9 to 14 m from each other. Sediment sampling locations were near the wetland centers, rather than being located in areas of hydrologic inputs or outputs (Windham-Myers et al., in this issue-a).

While the specific management of individual rice fields varied, as determined by the farmer, the temporal sampling design focused on three general periods defined by the rice management schedule: a) the rice growing season (June through August), during which time the rice growing fields were flooded; b) the water drawdown/ harvest period (September through November); and c) the post-harvest period (November through February) when fields were re-flooded to decay remaining rice straw. There were six sediment sampling events between June 2007 and February 2008. During the first sampling event (June 2007) two separate sites, 90 to 290 m apart, were sampled within each wetland to examine within-field variability. Only one of the two sites per wetland was revisited during subsequent sampling events. To increase the number of non-agricultural sites, and for comparison to PW5-ow, site PW2 was added during the last two sampling events. Table S1 (Supplemental Information) summarizes the sampling schedule and the hydrologic status of each wetland. A site map and further details on the study area, hydrology, wetland management schedule and project sampling schedule are detailed elsewhere (Windham-Myers et al., in this issue-a).

The surface 0 to 2 cm depth interval of sediment was sampled and preserved on ice as previously described (Marvin-DiPasquale et al., 2009a). Further sub-sampling was conducted at the USGS laboratory in Menlo Park, CA, 1 to 2 days after field collection. Field parameters measured included sediment temperature, pH, and E_h (oxidation–reduction potential) (Marvin-DiPasquale et al., 2009a). In rice growing fields, rice plant roots were concentrated in the surface 0 to 2 cm interval sampled during the peak of the growing season (L. Windham, personal communication)

and decreased in biomass to a depth of approximately 20 to 30 cm (Windham-Myers et al., in this issue-c). In addition to the above sampling schedule, Fields #32 and #65 (both managed as wild rice fields during June 2007 thru February 2008) were re-sampled for Hg-speciation only during July 2008, while fully dry and being held as fallow fields for the 2008 growing season.

2.2. Laboratory analyses

Sediment and pore-water were sub-sampled in the laboratory under anaerobic conditions (Marvin-DiPasquale et al., 2009a). Pore-water was initially extracted via centrifugation and subsequently filtered (0.45 µm nylon filter). Table 1 summarizes the sediment and pore-water parameters measured, the notation used in the remainder of this report, and the methods used. Samples that were incubated for MPP and SR rates were incubated in parallel at the average field temperature (± 1 °C) for that sampling event. Details regarding the $^{203}\text{Hg}(\text{II})$ radiotracer amendment incubations used to measure the Hg(II)-methylation rate constant (k_{meth}) are given as Supplemental Information (Section A). A summary of quality control and assurance measurements for all analytes listed in Table 1 is given as Supplemental Information (Section B), including information regarding holding times, method detection limits, method blanks, field duplicates, analytical duplicates, matrix spike recoveries, and certified reference material recoveries.

The one method not detailed in the references provided in Table 1 relates to the measurement of stable sulfur isotopes of pore-water sulfate ($\text{pw}[\delta^{34}\text{S}\text{SO}_4^{2-}]$), which is described here. Pore-water was initially sub-sampled into crimp-sealed vials under anaerobic conditions and preserved frozen. Upon thawing, samples were acidified with HCl to a pH of 3 to 4, stripped of dissolved sulfide with nitrogen gas, and diluted with deionized water. Dissolved pore-water sulfate ($\text{pw}[\text{SO}_4^{2-}]$) was precipitated as barium sulfate by the addition of excess barium chloride. The precipitate was filtered onto 0.45 µm cellulose acetate membrane filters, dried at 50 °C, and transferred into borosilicate

glass vials until further processing (Carmody et al., 1998). Precipitate subsamples (ca. 0.35 mg) were transferred into 5 × 9 mm tin capsules, amended with approximately 2 mg of vanadium pentoxide, and crimp sealed. Samples were then combusted and analyzed for stable S isotope composition (Giesemann et al., 1994) using a Costech Analytical Inc. elemental analyzer (model ECS4010) coupled to a Thermo-Finnigan Delta Plus XP mass spectrometer operated in continuous flow mode. Stable isotope compositions are expressed in delta (δ) notation as per mil (‰) deviations relative to a standard:

$$\delta^{34}\text{S} = \left(R_{\text{sample}}/R_{\text{standard}} \right) - 1 \quad (1)$$

where R refers to the $^{34}\text{S}/^{32}\text{S}$ isotope ratio. Values of $\delta^{34}\text{S}$ are expressed relative to the Vienna-Cañon Diablo Troilite (V-CDT) by normalization using primary sulfate standards (IAEA-SO-6 = -34.1% , NBS127 = 21.1%); precision was $\pm 0.2\%$. For a number of samples, the $\text{pw}[\text{SO}_4^{2-}]$ concentration was too low for $\delta^{34}\text{S}$ measurement.

2.3. Statistics

Data were analyzed using TICBO Spotfire S+ (version 8.1) statistical software. Type II error probability was set at $p < 0.05$ for all statistical tests, unless otherwise noted. The two-sided Kolmogorov-Smirnov 'goodness of fit' test was performed on the residuals for each parameter listed in Table 1, and indicated that a minority (30%) were normally distributed. Logarithmic (base 10; LOG_{10}) transformation increased this to 65%, with the remaining 35% of all parameters still being not normally distributed. Thus, median and interquartile ranges (IQR; 25th–75th percentile range) are generally reported. LOG_{10} transformed data were used, when appropriate, for Pearson's correlation (correlation coefficient reported as r_p) and regression analysis only. The non-parametric Wilcoxon Rank Sum (WRS) test was used on non-transformed data (only) to compare medians for data grouped by habitat type (agricultural vs. non-agricultural wetlands) and by time period in

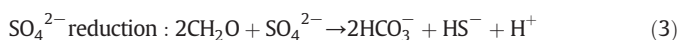
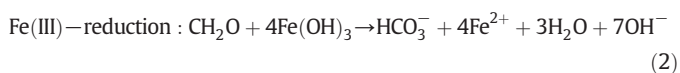
Table 1
Methods summary for sediment and pore-water parameters.

Notation	Analyte	Method citation
<i>Sediment mercury parameters</i>		
THg	Total mercury	Marvin-DiPasquale et al. (2011)
MeHg	Methylmercury	Marvin-DiPasquale et al. (2011)
$\text{Hg}(\text{II})_{\text{R}}$	Inorganic reactive mercury	Marvin-DiPasquale et al. (2011)
k_{meth}	MeHg production potential rate constant via $^{203}\text{Hg}(\text{II})$ amendment incubation	Marvin-DiPasquale et al. (2003a)
MPP	MeHg production potential rate (calculated)	Marvin-DiPasquale et al. (2011)
<i>Sediment non-mercury parameters</i>		
SR	Microbial sulfate reduction rate	Marvin-DiPasquale et al. (2008)
AVS	Acid volatile sulfur	Marvin-DiPasquale et al. (2008)
TRS	Total reduced sulfur	Marvin-DiPasquale et al. (2008)
$\text{Fe}(\text{II})_{\text{AE}}$	Acid extractable ferrous iron [Fe(II)]	Marvin-DiPasquale et al. (2008)
$\text{Fe}(\text{III})_{\text{a}}$	Amorphous (poorly crystalline) ferric iron [Fe(III)]	Marvin-DiPasquale et al. (2008)
$\text{Fe}(\text{III})_{\text{c}}$	Crystalline ferric iron [Fe(III)]	Marvin-DiPasquale et al. (2008)
%LOI	Percent weight loss on ignition	Marvin-DiPasquale et al. (2008)
GS	Grain size ($\% < 63 \mu\text{m}$)	Matthes et al. (1992)
E_{h}	Oxidation–reduction potential	Marvin-DiPasquale et al. (2008)
pH	pH	Marvin-DiPasquale et al. (2008)
<i>Pore-water parameters</i>		
$\text{pw}[\delta^{34}\text{S}\text{SO}_4]$	$^{34}\text{S}/^{32}\text{S}$ isotope ratio in aqueous sulfate relative to the Vienna-Cañon Diablo Troilite (V-CDT) standard	See text
$\text{pw}[\text{SO}_4^{2-}]$	Sulfate	Marvin-DiPasquale et al. (2008)
$\text{pw}[\text{Cl}^-]$	Chloride	Marvin-DiPasquale et al. (2008)
$\text{pw}[\text{Fe}(\text{II})]$	Ferrous iron [Fe(II)]	Marvin-DiPasquale et al. (2008)
$\text{pw}[\text{DOC}]$	Dissolved organic carbon	Marvin-DiPasquale et al. (2009a)
$\text{pw}[\text{H}_2\text{S}]$	Sulfide	Marvin-DiPasquale et al. (2009a)
$\text{pw}[\text{ALK}]$	Bicarbonate alkalinity (HCO_3^-)	Marvin-DiPasquale et al. (2009a)
$\text{pw}[\text{Ac}]$	Acetate	Windham-Myers et al. (2009)

agricultural wetlands (growing season [June–August] vs. the post-harvest period [December–February]). In cases where left-censored (less than reporting limit) data existed for a given parameter, summary statistics (medians and IQRs) were calculated on non-transformed data using ‘maximum likelihood estimation’ (Helsel, 2005) sub-routines developed by the USGS for the S+ statistical platform.

2.4. Assessing time integrated microbial iron and sulfate reduction rates

Although SR rate measurements via short-term radiotracer (i.e. $^{35}\text{SO}_4^{2-}$) incubation have long been a standard approach for assessing this microbial process in aquatic systems (Jørgensen, 1978), and were used in this study, a parallel approach for assessing rates of microbial FeR via short-term radiotracer amendments has proven problematic due to very rapid abiotic back-reactions associated with Fe(II) oxidation (Roden and Lovley, 1993). An alternative approach was thus used both to estimate net Fe(III) reduction (and Fe(II) oxidation) and to compare apparent net rates of FeR and SR more directly at our study sites. Site-specific, average daily rates of change for all sediment and pore-water Fe and S species concentrations were calculated for the period between each two successive sampling dates to assess all net changes in Fe(III)-reduction, Fe(II)-oxidation, SO_4^{2-} reduction and S^{2-} oxidation. Concentration changes in all Fe and S pools were assumed to encompass both microbial and abiotic reactions. After considering the rate data for all pools (See Section 3.3), it was decided that average daily rates of bulk sediment total ferric iron (Fe(III)_T) decrease and total reduced sulfur (TRS) increase would be used for estimating C-flow through microbial FeR and SR, respectively, using the generalized stoichiometry (Finke et al., 2007):



where CH_2O represents generic organic matter.

3. Results and discussion

The sediment microbiology and biogeochemistry associated with rice growing wetlands has been an area of active research for decades (Kirk, 2004), with much of this research focused on the rhizosphere zone as it relates to Fe chemistry (Begg et al., 1994; Kirk and Bajita, 1995), nutrients (Kirk and Du, 1997; Kirk, 2003; Klüber and Conrad, 1998 (Kirk and Du), methane production and oxidation (Chanton et al., 1997; vanderGon and Neue, 1996), and the competition among terminal electron accepting microbial processes (Achtlich et al., 1995; Bodegom and Stams, 1999; Liesack et al., 2000; Reichardt et al., 1997). Only recently has attention begun to be focused on the role of rice agriculture as it relates to biogeochemistry and ecological implications of potentially toxic metals such as selenium (Fang et al., 2010), cadmium (Liu et al., 2010), arsenic (Liang et al., 2010; Yun et al., 2010) and mercury (Ackerman and Eagles-Smith, 2010; Ackerman et al., 2010; Feng et al., 2008; Meng et al., 2010; Rothenberg and Feng, 2012; Rothenberg et al., 2011; Rothenberg et al., 2012; Shi et al., 2005; Zhang et al., 2010).

Site-specific non-parametric summary statistics (median, IQR, and the number of observations) for all analytical parameters are given as Supplemental Information (Tables S2a and S2b). Site-specific average daily rates of changes between consecutive sampling events and for defined study periods (e.g. the rice growing season) are presented for all Hg metrics (Table S3) and for all redox-sensitive Fe (Table S4) and S (Table S5) species as Supplemental Information.

3.1. Spatial and temporal trends of mercury metrics

Non-parametric WRS test results of spatial (agricultural vs. non-agricultural wetlands) and temporal (growing vs. post-harvest season) comparison of medians between paired groupings are given in Tables 2 and 3, respectively. Mercury parameters (including THg, Hg(II)_R , k_{meth} , MeHg, and MPP) are plotted by habitat type and in time series to illustrate both spatial and temporal data trends (Supplemental Information Fig. S1A–S1E, respectively).

Although sediment THg concentration varied little over time at any given site, there were differences among habitat types (Fig. S1A). Agricultural wetlands had significantly more THg in surface sediment than non-agricultural wetlands (Table 2). This difference in THg concentration was at least partially due to an east–west gradient in THg, with concentrations increasing approximately 4-fold overall from east to west (Supplemental Information Fig. S2). However, there was no statistically significant east–west gradient (least-squared regression slopes for THg vs. Longitude plots not significantly different from zero) when grouped solely by agricultural or by non-agricultural habitat type (not shown). Instead there appeared to be a marked increase in THg concentration west of -121.603° longitude, with a more than 2-fold higher THg concentrations in the agricultural wetlands (west) than the non-agricultural wetlands (east) (Table 2). There were no significant differences in THg concentration among agricultural wetlands grouped by season (growing vs. post-harvest, Table 3).

Agricultural wetlands had significantly higher (>20-fold) sediment Hg(II)_R concentrations than did non-agricultural wetlands (Table 2, Fig. S1B). During the June–August growing season, Hg(II)_R concentrations decreased in agricultural wetlands, followed by an increase during August–December, when the fields were drained and rice harvested. During the December–February post-harvest and reflooding period, Hg(II)_R concentrations again decreased. There were no significant differences in Hg(II)_R concentration among agricultural wetlands grouped by season (Table 3). However, the mean Hg(II)_R concentration for the dry and fallow fields #32 and #65 during July 2008 ($15.8 \pm 1.0 \text{ ng g}^{-1}$ dry wt., $n = 6$) was 3-fold greater (ANOVA, $P < 0.0001$) than during July 2007 ($4.8 \pm 0.9 \text{ ng g}^{-1}$ dry wt., $n = 2$), when the same two fields were wetted and being managed for wild rice (Fig. S1B), even though THg concentrations were similar for these two fields during July 2007 ($338 \pm 37 \text{ ng g}^{-1}$ dry wt., $n = 2$) and July 2008 ($317 \pm 54 \text{ ng g}^{-1}$ dry wt., $n = 6$) (Fig. S1A). In fact, the Hg(II)_R concentrations associated with the samples collected during July 2008 (range = 14.0 to 17.1 ng g^{-1} dry wt., $n = 6$) were higher than any of the samples collected from any site during the principal study period (June 2007 thru February 2008). This suggests that periods of wetland drying were also associated with an increase in Hg(II) availability, although the microbes associated with Hg(II) -methylation were very likely not active during periods of desiccation and soil oxidation.

Both spatial and temporal trends in sediment Hg(II)_R concentration were largely the mirror opposite of trends in k_{meth} , particularly for agricultural fields (cf. Figs. S1B and S1C). Across all sites and dates, $\text{LOG}_{10}[k_{\text{meth}}]$ and $\text{LOG}_{10}[\text{Hg(II)}_R]$ concentration exhibited a strong negative correlation ($r_p = -0.74$, $p < 0.001$, Fig. 1). Median values of k_{meth} were significantly higher (ca. 15-fold) in non-agricultural wetlands compared to agricultural wetlands (Table 2). After initially increasing throughout the growing season (June–August), k_{meth} values in most fields decreased during the August–December period, when agricultural wetlands were drained and rice harvested, and then increased again during December–February, particularly for the white rice fields (Supplemental Information, Table S3 and Fig. S1C). There were no significant differences in k_{meth} values among agricultural wetlands grouped by season (Table 3).

Because MPP rates are a function of both k_{meth} and Hg(II)_R , opposing spatial and temporal trends for these two parameters (Fig. 1), resulted in MPP rates that were similar among wetland types throughout most of the year (Fig. S1D). There was no significant difference between agricultural and non-agricultural wetlands (Table 2) or between growing

Table 2

Wilcoxon rank sum results comparing sediment and pore-water data grouped as agricultural versus non-agricultural wetlands. [The non-parametric Wilcoxon rank sum (WRS) comparison of medians included all sites and sampling dates. The first quartile (Q1, 25th percentile), median (50th percentile), third quartile (Q3, 75th percentile) and the number of observations (N) are shown, along with all results from mercury metric comparisons. Only significant results for non-mercury metrics are shown. Significant differences between groupings at probability levels of $p < 0.05$ and $p < 0.10$ are indicated as '****' and '**', respectively. Non-significant differences are indicated as 'NS'. Parameter notation defined in Table 2.]

Parameter	(units)	Agricultural				Non-Agricultural				WRS
		25th %	Median	75th %	N	25th %	Median	75th %	N	
<i>Sediment mercury parameters</i>										
THg	(ng g ⁻¹) dry wt.	300	330	377	(36)	128	142	154	(20)	***
Hg(II) _R	(ng g ⁻¹) dry wt.	1.06	4.37	8.57	(36)	0.14	0.20	0.25	(20)	***
%Hg(II) _R	(% of THg)	0.32	1.33	2.39	(36)	0.11	0.14	0.20	(20)	***
MeHg	(ng g ⁻¹) dry wt.	1.80	2.24	2.98	(36)	1.30	1.49	2.35	(20)	***
%MeHg	(% of THg)	0.52	0.73	1.00	(36)	0.90	1.04	1.42	(20)	***
k _{meth} ^a	(d ⁻¹)	6.4 × 10 ⁻⁴	9.9 × 10 ⁻³	8.8 × 10 ⁻²	(36)	6.7 × 10 ⁻²	1.5 × 10 ⁻¹	4.3 × 10 ⁻¹	(20)	***
MPP rate ^a	(pg g ⁻¹ d ⁻¹) dry wt.	4.5	29.7	88.9	(36)	9.8	29.6	48.5	(20)	NS
<i>Sediment non-mercury parameters</i>										
AVS	(μmol g ⁻¹) dry wt.	0.36	0.79	4.43	(36)	7.36	12.86	25.32	(20)	***
TRS	(μmol g ⁻¹) dry wt.	0.95	2.13	4.80	(36)	13.6	21.6	35.3	(20)	***
SR rate	(pg g ⁻¹) dry wt.	4.3	10.8	30.0	(35)	14.0	25.7	44.1	(20)	*
Fe(II) _{AE}	(mg g ⁻¹) dry wt.	2.33	3.28	6.40	(36)	5.89	6.94	7.68	(20)	***
Fe(II) _a ^a	(mg g ⁻¹) dry wt.	0.44	0.53	0.77	(36)	0.014	0.031	0.063	(20)	***
Fe(III) _c	(mg g ⁻¹) dry wt.	10.7	13.1	15.6	(36)	4.26	5.72	7.20	(20)	***
Fe _T ^b	(mg g ⁻¹) dry wt.	16.6	17.8	18.9	(36)	11.3	12.9	14.1	(20)	***
%Fe(II) _{AE} ^c	(% of Fe _T)	12.1	19.5	38.4	(36)	45.7	57.0	60.2	(20)	***
%LOI	(% of dry wt.)	6.4	6.8	7.3	(36)	6.9	8.1	9.6	(20)	***
GS	(% <63 μm)	70	78	89	(36)	56	63	80	(20)	***
E _n Field	(mv)	67	149	202	(35)	-2	40	81	(19)	***
E _n Lab	(mv)	-33	76	155	(36)	-96	-1	22	(20)	***
Bulk density	(g cm ⁻³) wet wt.	1.47	1.51	1.53	(36)	1.30	1.39	1.44	(20)	***
Dry wt.	(% of wet wt.)	57.5	58.7	60.7	(36)	40.0	50.2	55.6	(20)	***
Porosity	(mL cm ⁻³)	0.59	0.62	0.64	(36)	0.64	0.70	0.76	(20)	***
<i>Pore-water non-mercury parameters</i>										
pw[SO ₄ ²⁻]	(mmol L ⁻¹)	0.44	0.89	1.60	(36)	0.01	0.10	0.35	(20)	***
pw[Cl ⁻]	(mmol L ⁻¹)	2.64	3.52	4.40	(36)	1.28	1.96	2.54	(20)	***
pw[SO ₄ ²⁻ /Cl ⁻]	(unitless)	0.18	0.27	0.38	(36)	0.00	0.06	0.20	(20)	***
pw[δ ³⁴ S _{SO4}]	(‰, V-CDT)	0.38	3.68	10.71	(28)	3.88	13.85	17.99	(8)	*
pw[Fe(II)] ^a	(mg L ⁻¹)	0.005	0.055	0.31	(36)	0.19	0.47	1.00	(20)	***
pw[ALK]	(mg L ⁻¹) as HCO ₃ ⁻	485	542	668	(33)	347	418	522	(20)	***
pw[DOC]	(mg L ⁻¹) as C	14.0	19.0	24.9	(34)	10.5	12.0	15.5	(20)	***

^a Parameter contains left-censored (less than) data. Quartiles calculated using 'maximum likelihood estimate' statistics (Helsel, 2005).

^b Total Iron (Fe_T); calculated as Fe_T = Fe(II)_{AE} + Fe(III)_a + Fe(III)_c.

^c Percentage of Fe_T as Fe(II)_{AE} (%Fe(II)_{AE}); calculated as %Fe(II)_{AE} = Fe(II)_{AE}/Fe_T × 100.

Table 3

Wilcoxon rank sum results comparing sediment and pore-water data from agricultural wetlands grouped as growing season versus post-harvest season. [The non-parametric Wilcoxon rank sum (WRS) comparison of medians included all sampling dates and agricultural wetlands (only). The first quartile (Q1, 25th percentile), median (50th percentile), third quartile (Q3, 75th percentile) and the number of observations (N) are shown, along with all results from mercury metric comparisons. Only significant results for non-mercury metrics are shown. Significant differences between groupings at probability levels of $p < 0.05$ and $p < 0.10$ are indicated as '****' and '**', respectively. Non-significant differences are indicated as 'NS'. Parameter notation defined in Table 1.]

Parameter	(units)	Growing Season				Post-Harvest				WRS
		25th %	Median	75th %	N	25th %	Median	75th %	N	
<i>Sediment mercury parameters</i>										
THg	(ng g ⁻¹) dry wt.	301	345	378	(22)	300	324	367	(14)	NS
Hg(II) _R	(ng g ⁻¹) dry wt.	0.90	2.84	7.52	(22)	3.44	4.84	9.40	(14)	NS
%Hg(II) _R	(% of THg)	0.25	1.04	2.16	(22)	1.00	1.62	2.80	(14)	NS
MeHg	(ng g ⁻¹) dry wt.	1.49	1.94	2.26	(22)	2.53	3.17	4.06	(14)	***
%MeHg	(% of THg)	0.39	0.56	0.82	(22)	0.72	1.01	1.07	(14)	***
k _{meth} ^a	(d ⁻¹)	6.4 × 10 ⁻⁴	1.3 × 10 ⁻²	7.0 × 10 ⁻²	(22)	6.5 × 10 ⁻⁴	6.5 × 10 ⁻³	1.1 × 10 ⁻¹	(14)	NS
MPP ^a	(pg g ⁻¹ d ⁻¹) dry wt.	4.5	22.1	88.7	(22)	4.5	35.7	94.0	(14)	NS
<i>Sediment non-mercury parameters</i>										
SR	(pg g ⁻¹) dry wt.	10.4	13.0	34.3	(21)	1.12	2.14	21.6	(14)	***
GS	(% <63 μm)	68	71	79	(22)	83	91	93	(14)	***
E _n Field	(mv)	63	103	175	(21)	143	192	293	(14)	*
E _n Lab	(mv)	-60	-26	133	(22)	58	111	201	(14)	***
bulk density	(g cm ⁻³) wet wt.	1.51	1.52	1.54	(22)	1.44	1.47	1.51	(14)	***
Porosity	(mL cm ⁻³) wet wt.	0.62	0.63	0.64	(22)	0.57	0.59	0.64	(14)	*
Temp Field	(°C)	19	23	28	(22)	10	12	15	(14)	***
<i>Pore-water non-mercury parameters</i>										
pw[Cl ⁻]	(mmol L ⁻¹)	3.1	4.0	4.9	(22)	1.1	2.6	4.1	(14)	***
pw[ALK]	(mg L ⁻¹) as HCO ₃ ⁻	531	602	677	(20)	423	508	524	(13)	***
pw[DOC]	(mmol L ⁻¹)	15.6	22.4	30.2	(20)	11.1	13.7	19.7	(14)	***

^a Parameter contains left-censored (less than) data. Quartiles calculated using 'maximum likelihood estimate' statistics (Helsel, 2005).

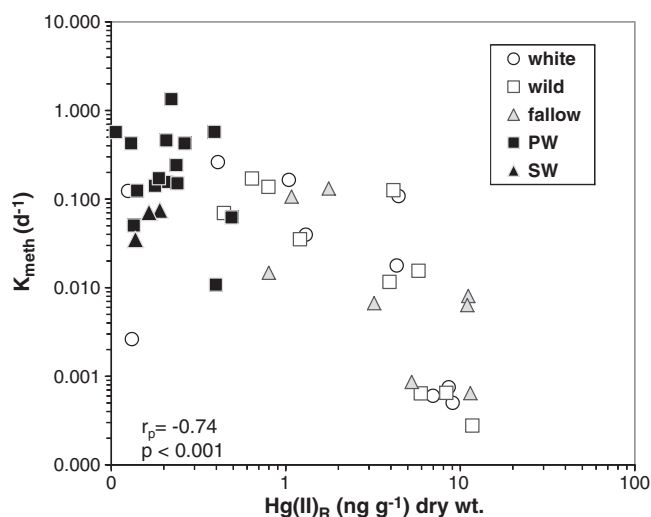


Fig. 1. Log–log plots of surface sediment (0–2 cm) reactive inorganic mercury (Hg(II)_R) concentration versus the $^{203}\text{Hg(II)}$ -methylation rate constant (k_{meth}). The Pearson product correlation coefficient (r_p) and probability (p) are given.

and post-harvest seasons (Table 3). The exception to this otherwise unremarkable suite of trends was during the post-harvest season, when MPP rates for wild rice fields peaked during December ($167 \pm 161 \text{ pg g}^{-1} \text{ d}^{-1}$, dry wt.; $n = 3$) and those for white rice fields peaked during February ($274 \pm 180 \text{ pg g}^{-1} \text{ d}^{-1}$, dry wt.; $n = 2$) (Fig. S1D). In contrast to MPP, sediment MeHg concentrations (and %MeHg) were significantly different by habitat type (agricultural > non-agricultural wetlands; Table 2 and Fig. S1E), and season (post-harvest > growing season; Table 3).

Samples collected during July 2008 from the dry fallow fields had a mean sediment MeHg concentration ($3.19 \pm 1.60 \text{ ng g}^{-1}$ dry wt., $n = 6$) that was approximately twice that measured for the same two fields during July 2007 ($1.62 \pm 0.15 \text{ ng g}^{-1}$ dry wt., $n = 2$), while flooded and being managed for wild rice production (Fig. S1E). The July 2008 mean MeHg concentrations were also higher than at any other time these two fields were sampled, except for during February 2008 ($5.16 \pm 1.01 \text{ ng g}^{-1}$ dry wt., $n = 2$) (Fig. S1E). It seems a likely scenario that between February and July 2008, when fields #32 and #65 were transitioned from wild rice to fallow and allowed to dry, some degree of net MeHg degradation occurred, but that a substantial fraction of the MeHg formed during the winter months was ultimately preserved in the desiccated sediment. Thus, the previous report of a sharp increase in surface water MeHg within days of reflooding managed wetlands within the Yolo Bypass (Marvin-DiPasquale et al., 2009a) may be accounted for by either a) the rapid release of MeHg formed during the previous wet period and preserved in dried sediment, b) a rapid response of microbial activity to reflooding, associated with the production of new MeHg produced from the elevated Hg(II)_R pool measured in the same dried substrate collected during July 2008 (as noted above), or c) some combination of these two processes. A similar spike in sediment MeHg concentrations after the rewetting of previously dried rice paddy soil was also reported by Rothenberg and Feng (2012).

3.2. Spatial and temporal trends of non-mercury metrics

Of the many non-mercury sediment and pore-water parameters measured (Table 1), those discussed in detail below appear the most relevant with respect to understanding and describing what controls Hg(II) -methylation among the habitat types studied. These key parameters are plotted in time-series graphs, by habitat type, to illustrate both spatial and temporal trends associated with S (Supplemental Information, Fig. S3A–S3F), Fe (Fig. S4A–S4D), and C chemistry along with sediment E_h and pH (Fig. S5A–S5F).

3.2.1. Sulfur chemistry

Median $\text{pw}[\text{SO}_4^{2-}]$ was significantly higher (>9-fold) in agricultural wetlands than in non-agricultural wetlands (Table 2; Fig. S3A). This difference is at least partially explained by the fact that the agricultural wetlands routinely receive fertilizer amendments, in the form of ammonium sulfate ($(\text{NH}_4)_2\text{SO}_4$) and zinc sulfate (ZnSO_4), when in rice production. For the current study sites, the white and wild rice fields received one application of sulfate-bearing fertilizers just days prior to our first sampling event in June 2007, a second application to the white rice fields 1 to 2 weeks prior to the second sampling event (July 2007), and a second application to the wild rice fields immediately following the July 2007 sampling. The fallow fields received no fertilizer amendment during our study. With a fertilizer application rate of approximately 337 to 421 kg per hectare (Jack DeWit, rice farmer, personal communication), this corresponds to a sulfate application rate of approximately 119 to 268 kg SO_4^{2-} per hectare for the white and wild rice fields during the study period (for more detail, see Alpers et al., this issue).

For both the white rice fields and the permanently flooded wetlands, the dominant seasonal pattern in $\text{pw}[\text{SO}_4^{2-}]$ included a decrease during the growing season, an increase during the draining/harvest period, and a decrease again during the post-harvest winter period (Fig. S3A). However, for both wild rice and fallow fields $\text{pw}[\text{SO}_4^{2-}]$ increased from the beginning of the growing season (June) until after the draining/harvest period (December), and then sharply decreased during the post-harvest (December–February) period. Although the observed increase in $\text{pw}[\text{SO}_4^{2-}]$ from June–December in the wild rice fields may be explained by the fertilizer application described above, this trend is in contrast to what was observed for the similarly amended white rice fields, and would not explain the rise in $\text{pw}[\text{SO}_4^{2-}]$ for the (non-fertilized) fallow fields. An alternative explanation is that the increase in salinity observed in the wild rice fields during the growing season, as evidenced by pore-water chloride ($\text{pw}[\text{Cl}^-]$) data (not shown), reflect very high rates of transpiration through the rice plants during the growing season (Bachand et al., this issue; Windham-Myers et al., in this issue-b), which drove a commensurate increase in $\text{pw}[\text{SO}_4^{2-}]$.

Because Cl^- is a conservative element in the environment, affected primarily by dilution and evaporative concentration, the pore-water sulfate-to-chloride molar ratio ($\text{pw}[\text{SO}_4^{2-}/\text{Cl}^-]$) allows us to separate changes in $\text{pw}[\text{SO}_4^{2-}]$ concentration due to microbiological and abiotic chemical reactions from those based solely on physical dilution or evaporative concentration (Marvin-DiPasquale et al., 2003b). The time-series plot of the $\text{pw}[\text{SO}_4^{2-}/\text{Cl}^-]$ ratio data (Fig. S3B) more clearly shows the relative changes in $\text{pw}[\text{SO}_4^{2-}]$ due to microbiological and/or abiotic reactions, with both white and wild rice fields exhibiting a general decrease during the growing season, indicative of microbial SR. All agricultural wetlands showed a marked increase during August to December, which suggests the oxidation of reduced-S compounds during the draining period. This was followed by a marked decrease in the $\text{pw}[\text{SO}_4^{2-}/\text{Cl}^-]$ ratio during December to February for all agricultural wetlands, which is consistent with a second period of enhanced SR during the post-harvest period.

The pore-water sulfide ($\text{pw}[\text{H}_2\text{S}]$) and elevated sediment TRS concentrations are considered indicative of past or current microbial SR activity. Although both were present, $\text{pw}[\text{H}_2\text{S}]$ was uniformly low for all sites and sampling dates, rarely exceeding $2 \mu\text{mol L}^{-1}$ (Fig. S3C). This suggests either rapid sulfide oxidation or precipitation into solid-phase Fe–S minerals. There were no significant differences (WRS test) in $\text{pw}[\text{H}_2\text{S}]$ among wetlands grouped by habitat or by season. In contrast, the seasonal pattern in TRS among all agricultural wetlands (as well as the permanent wetland) included an increase during the growing season, a decrease during the draining period, and a second increase during the post-harvest winter period (Fig. S3D); a pattern that was the mirror opposite of $\text{pw}[\text{SO}_4^{2-}/\text{Cl}^-]$ (Fig. S3B) and sediment E_h (Fig. S5E), with agricultural wetland TRS negatively correlated with both $\text{pw}[\text{SO}_4^{2-}/\text{Cl}^-]$ ($r_p = -0.59$, $p < 0.0001$) and field E_h ($r_p = -0.54$, $p < 0.001$). Median concentrations of TRS and acid-

volatile sulfur (AVS) (not shown in time-series) were significantly higher (ca. 10-fold) in non-agricultural wetlands as compared to agricultural wetlands (Table 2). No significant differences in TRS or AVS concentrations were found when data were grouped by season (WRS test).

Similar to the seasonal trend in sediment TRS concentration, SR rates were higher in non-agricultural wetlands (ca. 2-fold) compared to agricultural wetlands (Table 2, Fig. S3E). Temporally, SR rates in agricultural wetlands were significantly higher during the growing season (ca. 6-fold) compared to the post-harvest season, consistent with the temporal trend in field temperature (Table 3).

Greater SR in non-agricultural wetlands led to isotopically heavier (higher $\text{pw}[\delta^{34}\text{S}_{\text{SO}_4}]$) sulfate than in agricultural wetlands (Fig. 2 and Table 2). Sulfate reduction fractionates the isotopic composition of sulfate and sulfide such that during SR the residual (unused) pore-water sulfate becomes enriched in the heavy (^{34}S) isotope, whereas the reduced end-product (e.g. sulfide) is depleted in ^{34}S (Sharp, 2007). This interpretation is supported by the positive correlation between radiotracer derived SR rates and $\text{pw}[\delta^{34}\text{S}_{\text{SO}_4}]$ (Fig. 2A) and the negative correlation between the $\text{pw}[\text{SO}_4^{2-}/\text{Cl}^-]$ and $\text{pw}[\delta^{34}\text{S}_{\text{SO}_4}]$ (Fig. 2B). It is also noteworthy that $\text{pw}[\delta^{34}\text{S}_{\text{SO}_4}]$ values in the agricultural wetlands were in the range of values measured for the sulfur containing fertilizer applied to the fields (2.5–4.0‰ V-CDT, weighted average) during the beginning of the growing season (June–July). However, by the end of the growing season (August), both wild rice and white rice fields had $\text{pw}[\delta^{34}\text{S}_{\text{SO}_4}]$ values substantially higher (18–19‰ V-CDT) than this initial range, indicating active SR during that latter phase of crop growth (Fig. S3F).

The $\text{pw}[\delta^{34}\text{S}_{\text{SO}_4}]$ data also provide some evidence as to the extent of reduced-sulfur oxidation among the various habitat types. When reduced-sulfur compounds are oxidized back to SO_4^{2-} , the isotopic composition of the resulting SO_4^{2-} is similar to the parent reduced-sulfur compounds (i.e. little isotopic fractionation and low $\delta^{34}\text{S}$ value is largely retained) (Balci et al., 2007). The only instances of isotopically depleted $\text{pw}[\delta^{34}\text{S}_{\text{SO}_4}]$ (<0‰) occurred exclusively in agricultural wetlands, and only at sites with high E_h values (> +150 mv; Fig. 2C). This suggests that there is a substantial amount of reduced-sulfur oxidation that occurs within agricultural wetlands compared to non-agricultural wetlands, potentially related to routine annual soil tilling and harvest that is associated with agricultural fields. Collectively, these results indicate higher rates of microbial SR and a higher degree of reduced sulfur preservation (and less oxidation) in non-agricultural wetland sites, most likely from the precipitation of H_2S with dissolved iron to form Fe–S minerals.

The addition of SO_4^{2-} -bearing fertilizer did not appear to stimulate microbial SR. Non-fertilized wetlands had higher SR rates, compared to the agricultural wetlands, during the first two sampling events (June & July), and toward the end of the growing season (late August) the highest SR rates were observed in the non-fertilized fallow fields (Fig. S3E). Furthermore, $\text{pw}[\text{SO}_4^{2-}]$ in surface sediment associated with agricultural wetlands (including non-fertilized fallow fields) well exceeded the 0.03 mmol L^{-1} concentration threshold (Table S2a) above which SO_4^{2-} no longer limits microbial SR rates in freshwater systems (Lovley and Klug, 1986; Roden and Tuttle, 1993). Only in seasonal wetland and cattail-dominated permanent wetland sites were SO_4^{2-} concentrations below 0.03 mmol L^{-1} . This suggests that labile organic matter, rather than sulfate, limited SR rates in the 0–2 cm surface sediment of the agricultural wetlands studied during the growing season and post-harvest period.

3.2.2. Iron chemistry

Although the rate of microbial FeR was not measured directly, multiple iron pools were tracked throughout the study, which provides a dynamic picture of seasonal and spatial iron cycling. One measure of net FeR is the build-up of sediment acid-extractable ferrous iron ($\text{Fe}(\text{II})_{\text{AE}}$) concentration over time. Agricultural wetlands exhibited large seasonal

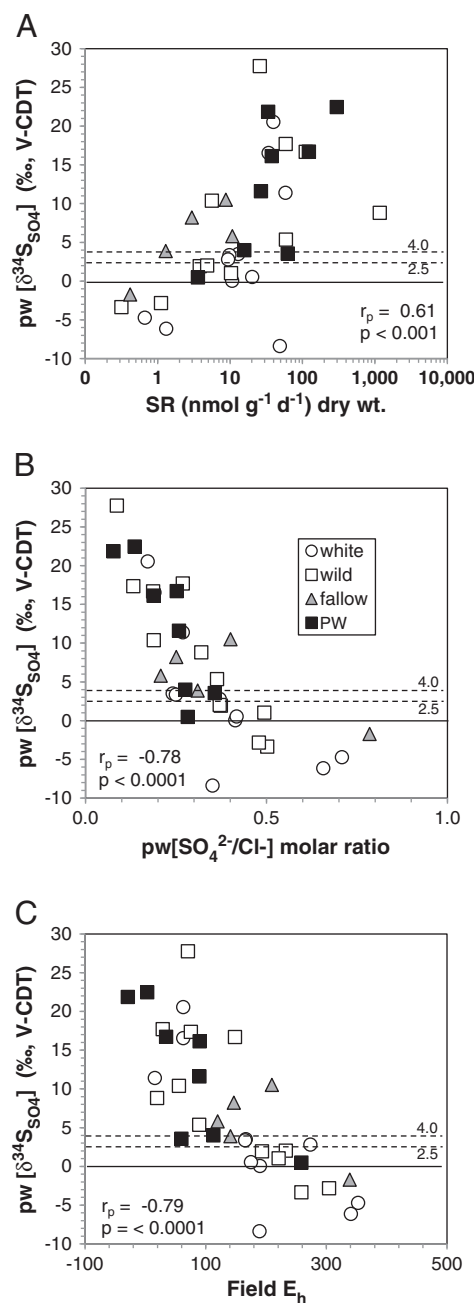


Fig. 2. X–Y plots of pore-water sulfate–sulfur stable isotope data ($\text{pw}[\delta^{34}\text{S}_{\text{SO}_4}]$) versus (A) sediment microbial sulfate reduction (SR) rate, (B) pore-water sulfate-to-chloride ($\text{pw}[\text{SO}_4^{2-}/\text{Cl}^-]$) molar ratio, and (C) sediment redox (E_h). Data from the June through December (2007) sampling period only, and is organized by habitat type (legend inset, PW = permanent wetland). The solid line indicates the $\text{pw}[\delta^{34}\text{S}_{\text{SO}_4}]$ zero value. The two dashed lines identify the lower and upper range of $\text{pw}[\delta^{34}\text{S}_{\text{SO}_4}]$ values (2.5–4.0‰, V-CDT, weighted averages) associated with fertilizer applied to wild rice and white rice fields during the 2007 growing season. The Pearson's correlation coefficient (r_p) and associated probability (p) is given in each panel.

changes in both pore water Fe(II) and sediment $\text{Fe}(\text{II})_{\text{AE}}$ concentrations (Figs. S4A and S4B), with both generally increasing during the growing and post-harvest seasons and decreasing during the interim draining/harvest period, likely reflecting the oxidation of Fe(II) back to Fe(III). The opposite temporal trend was observed for $\text{Fe}(\text{III})_{\text{a}}$ and $\text{Fe}(\text{III})_{\text{c}}$ concentrations (Figs. S4C and S4D), which generally decreased during the growing and post-harvest seasons and increased during the draining/harvest period in the agricultural wetlands. While total iron (Fe_T), $\text{Fe}(\text{III})_{\text{a}}$, and $\text{Fe}(\text{III})_{\text{c}}$ concentrations were all significantly higher in the agricultural wetlands, pore-water Fe(II) and sediment $\text{Fe}(\text{II})_{\text{AE}}$

concentrations were significantly higher in non-agricultural wetlands (Table 2). Although the temporal trends described above were evident in time series (Fig. S4), seasonal differences in agricultural wetlands were not significant for any of the Fe metrics (via the WRS test).

The temporal and spatial trend in the percentage of Fe_T that was Fe(II)_{AE} (%Fe(II)_{AE}) closely paralleled the trends in Fe(II)_{AE} (Figs. S4B and S4E). While the %Fe(II)_{AE} metric cannot be used to infer microbial rates, it can be interpreted as representing the continuum of sediment redox conditions ranging from one poised for FeR (as none of the Fe(III) has yet been reduced to Fe(II)), to one poised for microbial SR (as all of the Fe(III) has been reduced to Fe(II)), and thus provides a finite way to compare the relative redox status (based on Fe) of different sites and time points along the continuum. In this light, significantly lower %Fe(II)_{AE} values for the agricultural wetlands, compared to the non-agricultural wetlands (Table 2), would seem to suggest that the former are generally more poised for microbial FeR than the latter.

Previous studies (Lovley and Phillips, 1987b; Roden and Zachara, 1996) have shown that Fe(III)_a (amorphous Fe(III)) is more readily available to Fe(III)-reducing bacteria than Fe(III)_c (e.g. crystalline goethite (αFeOOH), hematite (Fe₂O₃), lepidocrocite (γFeOOH), and magnetite (Fe₃O₄)), due to the larger surface area of the amorphous form (Roden and Zachara, 1996). The concentration of Fe(III)_a also has been shown to be proportional to rates of microbial FeR (Roden and Wetzel, 2002). Thus, the higher concentrations of Fe(III)_a in the agricultural wetlands, compared to the non-agricultural wetlands, also suggest that the former were well suited for microbial FeR, particularly during the growing season.

3.2.3. Carbon chemistry, redox, and pH

Non-agricultural sites had greater median sediment organic matter concentration (as percent loss on ignition, %LOI), but lower pore-water dissolved organic carbon (pw[DOC]) and alkalinity (pw[ALK]), than did agricultural sites (Table 2; Fig. S5A, S5B, and S5D). There were no significant seasonal differences (WRS test) in %LOI in agricultural wetlands. In contrast, median concentrations of both pw[DOC] and pw[ALK] were significantly greater during the growing season than during the post-harvest season in agricultural wetlands (Table 3). This seasonal trend was particularly notable in the white and wild rice fields, where pw[DOC], pw[ALK], and pore-water acetate (pw[Ac]) all increased during the growing season and then decreased during the draining/harvest period (Fig. S5B, S5C, and S5D). However, it was during the post-harvest period (February) when the highest pw[Ac] concentrations (mean ≈ 1400 μmol L⁻¹) were observed in the white rice fields, which had an abundant amount of decaying rice straw (Fig. S5C). While pw[Ac] is only a minor subset of the total pw[DOC] pool, it is a key substrate for heterotrophic bacteria (including sulfate and iron reducers), and thus is a better proxy for the availability of low molecular weight organic compounds fueling heterotrophic bacteria than bulk DOC. The build-up of pw[Ac] during the growing season in agricultural wetlands is thought to reflect the release of acetate and fermentation precursors from live plants into soil (Windham-Myers et al., in this issue-c), followed by net acetate utilization by microbes during late summer and fall after rice harvest; a second spike during the post-harvest season likely represents acetate derived from decaying rice straw.

Sediment E_h changed dramatically throughout the study period in the agricultural wetlands (Fig. S5E), with a pattern similar to that for Hg(II)_R (Fig. S1B) and pw[SO₄²⁻/Cl⁻] (Fig. S3B): decreasing during the growing season, increasing during the draining/harvest period, and decreasing again during the post-harvest period. This seasonal trend in agricultural wetlands was the mirror opposite of that for k_{meth} (Fig. S1C), pw[H₂S] (Fig. S3C), TRS (Fig. S3D), pw[δ³⁴S₄²⁻] (Fig. S3F), and sediment Fe(II)_{AE} (Fig. S4B), illustrating how well the sediment E_h measurement tracks (or mirrors) individual redox-sensitive species. Agricultural wetlands were more oxidized (higher E_h) than non-agricultural wetlands (Table 2), and agricultural wetlands were more

reducing during the growing season compared to the post-harvest period (Table 3).

Sediment pH decreased modestly (0.1–0.3 pH units) both in rice growing fields and in the permanent wetland during the growing season (Fig. S5F), paralleling the increase in pw[Ac] (Fig. S5C) and likely reflected the increase in organic acids from fermentation reactions and/or plant root release (Windham-Myers et al., 2009; Windham-Myers et al., in this issue-c), or possibly the concurrent oxidation of Fe(II) associated with the rhizosphere (Kirk and Bajita, 1995), although sediment Fe(II)_{AE} exhibited a net increase during the growing season (Fig. S4B). This decrease in pH during the growing season was similar to the one reported by Rothenberg and Feng (2012) in their study of Hg cycling in rice fields in China. However, unlike E_h, there were no statistically significant spatial or temporal differences (WRS test) noted for sediment pH.

3.3. Net carbon flow through iron and sulfate reduction

In lieu of a reliable approach for assessing rates of microbial FeR via isotope-enriched short-term incubation, and to compare rates of FeR with those of SR more directly to assess the relative importance of these two processes on Hg cycling, a monthly-to-seasonal approach was taken, where average daily rates of change between subsequent sampling events were calculated for all Fe and S species and compared in common units (nmol g⁻¹ d⁻¹ dry wt.) (Supplemental Information Tables S4 and S5). This assessment in common units verified that solid phase constituents (i.e., sediment TRS, Fe(II)_{AE} and Fe(III)_T) exhibited much larger net changes over time than did pore-water constituents (i.e., pw[SO₄²⁻], pw[H₂S], and ferrous iron (pw[Fe(II)])), presumably because these dissolved pools are more readily affected by rapid oxidation reactions, and because they represent a small fraction of the bulk sediment pool (e.g. pw[H₂S] is a minor portion of sediment TRS). Pore-water constituents were thus excluded from consideration for the purposes of estimating C-flow through FeR and SR, and the increase in TRS was selected as the best parameter to estimate C-flow through the latter. Further, based on a detailed examination of temporal changes in sediment Fe(III)_T and Fe(II)_{AE} pools (Supplemental Information, Section C), it was concluded that oxidation-reduction reactions associated with these pools were fairly tightly coupled in surface sediment of the agricultural wetlands, and less so in the non-agricultural wetlands, and that the Fe(II)_{AE} pool is susceptible to more frequent back reactions than the Fe(III)_T pool on the monthly-seasonal time scale. Thus, bulk sediment Fe(III)_T depletion was determined to be the best candidate for estimating FeR rates.

Using the generalized stoichiometry for microbial FeR and SR (Eqs. (2) and (3)), daily rates of Fe(III)_T depletion and TRS increase (Tables S4 and S5) were converted to the common currency of generalized organic matter (CH₂O) oxidation for each time period and sub-habitat type (Table 4). A limitation of this approach is the inherent assumption that the periods of observed Fe(III)_T decrease and TRS increase are solely reflective of the heterotrophic microbial processes of FeR and SR, respectively, while in fact Fe(II) and H₂S oxidation reactions are very likely simultaneously occurring in the rhizosphere zone (Kirk and Bajita, 1995; Lee et al., 1999). To the extent that these oxidation reactions affect the observed net Fe(III)_T decrease or net TRS increase over time, the impact would be an underestimation of actual C-flow through microbial FeR and SR using the stoichiometric approach. However, a statistical (ANOVA) analysis indicated that SR rates estimated from long-term changes in the TRS pool compared reasonably well to those measured during short-term incubations with ³⁵SO₄²⁻ radiotracer, with no significant differences (p > 0.05) in the two approaches under most comparison scenarios (Supplemental Information, Section D). Because comparable short-term incubation data does not exist for FeR, the impact of Fe(II) oxidation reactions on the Fe(III)_T depletion calculation used for estimating FeR is unknown. However, to the extent that such back reactions may be comparable in effect to what was shown for SR estimates based upon TRS accumulation, and based on the fact that

Table 4

Estimated carbon flow through microbial iron and sulfate reduction. [Carbon flow through microbial iron reduction (FeR) and sulfate reduction (SR), was calculated for 0–2 cm surface sediment based on assumed stoichiometry (see text) and net Fe(III)_T decrease or net TRS increase, respectively, between consecutive sampling dates (normalized to daily rates). A period of net oxidation (OXID) was assumed (and C-flow not estimated) for periods of net Fe(III)_T increase or net TRS decrease. C-flow was also not determined (ND) when data from both consecutive sampling dates were not available. Data are organized by Site code, wetland type, and habitat (agricultural, AG; non-agricultural, non-AG). The propagated error term is given in parentheses ().]

Site	Type	Habitat	C-Flow	Carbon flow (nmol g ⁻¹ d ⁻¹) dry wt							
				Jun–Jul	Jul–Aug	Aug–Dec	Oct–Dec	Dec–Feb			
R31	White rice	AG	FeR	819	(136)	OXID		OXID	ND	109	
			SR	295	(56)	OXID		OXID	ND	407	(136)
R64	White rice	AG	FeR	OXID		444	(94)	OXID	ND	208	
			SR	11	(21)	175	(47)	OXID	ND	137	(18)
W32	Wild rice	AG	FeR	429	(68)	616	(187)	OXID	ND	147	
			SR	72	(56)	320	(44)	OXID	ND	59	(28)
W65	Wild rice	AG	FeR	443	(38)	170	(22)	262	(8)	ND	97
			SR	62	(19)	149	(73)	23	(46)	ND	182
F20	Fallow	AG	FeR	ND		643	(130)	OXID	ND	OXID	
			SR	ND		144	(31)	OXID	ND	19	(10)
F66	Fallow	AG	FeR	ND		304	(164)	OXID	ND	337	(1)
			SR	ND		316	(67)	OXID	ND	29	(12)
PW 5 OW	Permanent; Open-water	non-AG	FeR	406	(111)	OXID		27	(31)	ND	OXID
			SR	OXID		138	(85)	411	(63)	ND	OXID
PW 5 TUL	Permanent; Tule	non-AG	FeR	ND		OXID		6	(3)	ND	OXID
			SR	ND		OXID		OXID	ND	OXID	
PW 5 CAT	Permanent; Cattail	non-AG	FeR	ND		51	(106)	OXID	ND	OXID	
			SR	ND		OXID		OXID	ND	2049	(1550)
PW 2	Permanent; open-water	non-AG	FeR	ND		ND		ND	ND	OXID	
			SR	ND		ND		ND	ND	OXID	
SW G34N	Seasonal	non-AG	FeR	ND		ND		ND	562	OXID	
			SR	ND		ND		ND	174	(243)	66

Fe(III)_T depletion was explicitly selected because it appeared less susceptible to back reactions compared to the Fe(II)_{AE} pool (Supplemental Information, Section C), this approach to estimating and directly comparing SR and FeR rates based on monthly-seasonal changes in TRS and Fe(III)_T pools, respectively, is useful in trying to understand drivers of MeHg production in the wetland types studied.

For agricultural wetlands, C-flow was significantly (ANOVA, $p = 0.009$) greater through FeR (mean \pm std. err, 359 ± 59 nmol g⁻¹ d⁻¹, $n = 14$) compared to SR (150 ± 31 nmol g⁻¹ d⁻¹, $n = 16$), across all sites and periods for which C-flow was calculated. This trend was even more pronounced when limited to the growing season, with C-flow in agricultural fields again significantly (ANOVA, $p = 0.001$) greater through FeR (483 ± 72 nmol g⁻¹ d⁻¹, $n = 8$) compared to SR (171 ± 39 nmol g⁻¹ d⁻¹, $n = 9$). When considering the temporal trends in C-flow in the agricultural wetlands (only) through both FeR and SR combined, it is evident that C-flow through these terminal electron accepting processes was significantly greater (ANOVA, $p = 0.046$) during the growing season (632 ± 91 nmol g⁻¹ d⁻¹, $n = 9$) than during the post-harvest season (342 ± 52 nmol g⁻¹ d⁻¹, $n = 9$), which is consistent with the temporal trends in pw[ALK] and pw[DOC] (Table 3).

3.4. Controls on methylmercury production

Net MeHg production is ultimately a function of the availability of Hg(II) to the community of Hg(II)-methylating bacteria, and of the activity of those bacteria (Bridou et al., 2011; Marvin-DiPasquale et al., 2009b), as well as the rates of biotic (Marvin-DiPasquale et al., 2000) and abiotic (Sellers et al., 1996) processes that facilitate MeHg degradation. Setting aside MeHg degradation processes, it is useful to deconstruct the question regarding what controls MeHg production, at a given time or place, by asking: 1) What controls Hg(II) availability, and 2) What controls the activity of Hg(II)-methylating bacteria? In the current study we have attempted to address this by a) using available proxy measurements for both Hg(II) availability (i.e., the Hg(II)_R assay) and the activity of the Hg(II)-methylating community (i.e., the k_{meth} assay); b) using these independently measured parameters to calculate MPP rates; c) conducting a detailed examination of sediment geochemistry; d) examining microbial rates of both FeR and SR; and e)

examining a geochemically and hydrologically diverse suite of wetlands. It is important to note that this study was restricted to the uppermost 0–2 cm sediment interval, where microbial rates tend to be greatest and representing the narrow sediment zone that is in close physical and chemical communication with the surface water. However, oxidation–reduction reactions facilitated by plant root/soil interactions in the rhizosphere, which extends much deeper than the 0–2 cm interval, likely affect the vertical profiles for Hg speciation and Hg-transformation (Rothenberg and Feng, 2012) in ways not addressed in the current study.

One overarching trend seen both in this study and a previous investigation (Marvin-DiPasquale et al., 2009b) is that environmental conditions that lead to an increase in Hg(II)_R concentration tend to lead simultaneously to a decrease in k_{meth} , and vice versa (Fig. 1; cf. Fig. S1B and S1C). Correlation analysis of the complete data set demonstrated that TRS concentration was positively correlated with k_{meth} ($r_p = 0.88$) and negatively correlated with Hg(II)_R ($r_p = -0.79$) (Fig. 3). Sediment TRS was more strongly correlated with these two Hg parameters than were any of the Fe parameters.

For this suite of sites we conclude that the spatial–temporal variation in the activity of the Hg(II)-methylating bacterial consortium had a larger effect on the variability of the MPP rates than did the variation in Hg(II) availability, based on the 10,000-fold range in k_{meth} values compared to a 100-fold range in Hg(II)_R concentration for the complete dataset. This result is consistent with the findings from an earlier study of eight diverse stream-bed sediment environments (Marvin-DiPasquale et al., 2009b).

Iron speciation chemistry also provides unique insight into temporal changes in Hg(II)-availability and the activity of the Hg(II)-methylating community. Specifically, for all agricultural wetlands, during the period of net Fe(II)-oxidation (i.e. August–December), as the rate of Fe(II)-oxidation increased, k_{meth} decreased and at an increasing rate, while Hg(II) concentrations increased at an increasing rate (Fig. 4). Conversely, during periods of net FeR, as the FeR rate increased, k_{meth} increased at an increasing rate, while Hg(II) concentrations decreased at an increasing rate. However, the high degree of correlation between the rate (and direction) of change in Fe(II)_{AE} pools and k_{meth} ($r_p = 0.84$, $p < 0.0001$), and between the rate (and direction) of change in Fe(III)_T pools and Hg(II)_R concentration, does not imply causation.

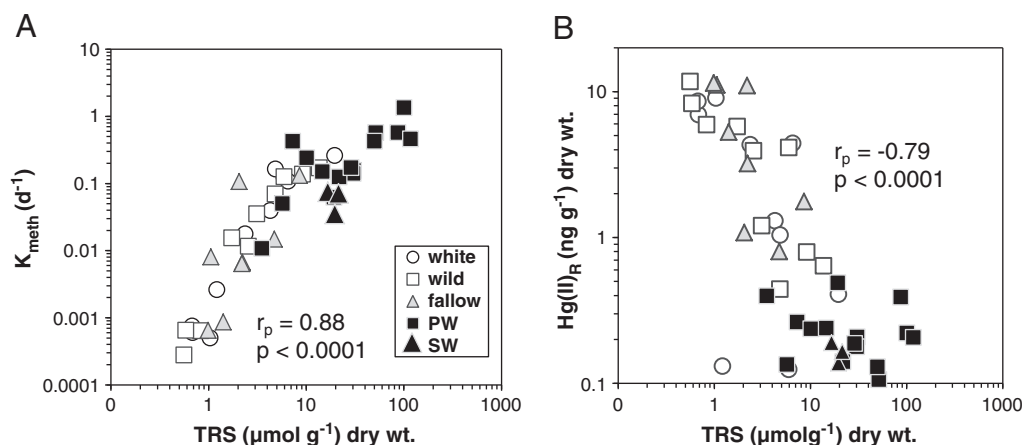


Fig. 3. Log-log plots of total reduced sulfur (TRS) versus the ²⁰³Hg(II)-methylation rate constant (k_{meth}) and reactive inorganic mercury (Hg(II)_R) concentration (panels A and B, respectively), by wetland type. The Pearson product correlation coefficient (r_p) and probability (p) are given in each case.

Indeed, a very similar trend and degree of correlation ($r_p = 0.83$, $p < 0.0001$) was observed when the rate of change in TRS concentration was plotted against k_{meth} (not shown). However, this novel approach to examining the changes in sediment geochemistry between sampling dates points to strong linkages between the biogeochemical cycling of Fe and Hg. Further, the above-noted positive correlation between increasing rates of FeR and k_{meth} is consistent with the hypothesis that

Fe(III)-reducing bacteria are involved to some degree with Hg(II)-methylation in the suite of agricultural wetlands examined. Finally, the above analysis of C-flow suggests that microbial FeR out-paced SR in the agricultural wetlands, particularly during the growing season (Table 2). Although the information regarding C-flow is less clear in the non-agricultural wetlands, it seems that SR exceeded FeR during the majority of the periods when the ‘integration-between-sampling-events’ approach was possible (Table 4). It is noteworthy that plots similar to those presented in Fig. 4 for non-agricultural wetlands (not shown) indicated weaker correlations driven by 1 to 2 data points; thus, the above-mentioned correlations do not hold true for non-agricultural sites, which were clearly not dominated by microbial FeR.

After deconstructing the MPP rate into its component parts, k_{meth} and Hg(II)_R , and examining respective controls, metrics for both microbial FeR and SR differed in their power for predicting MPP rates as a function of wetland setting. Specifically, as both $\text{Fe(II)}_{\text{AE}}$ and TRS concentration increased, MPP rates increased (Fig. 5). However, the slopes of these relationships were essentially constant in the case of $\text{Fe(II)}_{\text{AE}}$, and almost double in the case of TRS for the agricultural wetlands compared to the non-agricultural, permanently flooded wetlands. In other words, in terms of a metric for microbial FeR, as sediment $\text{Fe(II)}_{\text{AE}}$ concentrations increased there was a similar response in MPP rates in both agricultural and permanent wetlands, but with overall higher MPP rates in the agricultural wetlands (larger Y-intercept). In contrast, in terms of a metric for microbial SR, as sediment TRS concentrations increased, MPP rates increased, but at a faster rate in agricultural wetlands than in non-agricultural wetlands. Further, $\text{Fe(II)}_{\text{AE}}$ was only a slightly better predictor of MPP rates ($r^2 = 0.57$), compared to TRS ($r^2 = 0.52$), in agricultural wetlands. In contrast, TRS was a better predictor of MPP rates ($r^2 = 0.50$), compared to $\text{Fe(II)}_{\text{AE}}$ ($r^2 = 0.36$), in seasonal wetlands. These results are consistent with the hypothesis that both FeR and SR bacteria were involved in MeHg production in both agricultural and non-agricultural wetlands, but that substantial Fe(II) oxidation in the rhizosphere of rice growing wetlands (Begg et al., 1994; Kirk and

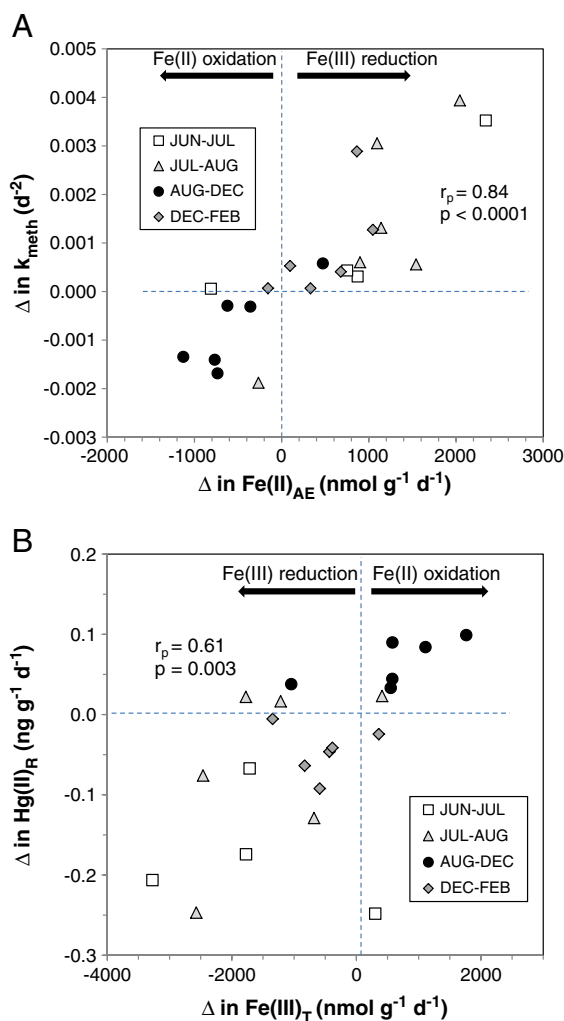


Fig. 4. X-Y plots of A) the daily rate of change (Δ) in the Hg(II)-methylation rate constant (k_{meth}) versus the Δ in acid-extractable ferrous iron ($\text{Fe(II)}_{\text{AE}}$), and B) the Δ in reactive mercury (Hg(II)_R) versus the Δ in total ferric iron (Fe(III)_T) concentration, in agricultural wetlands (only); where Δ is calculated as the difference between two subsequent sampling events (indicated by symbol style) divided by the number of days between the two events. The vertical and horizontal dashed lines indicate zero change for the parameters associated with the X and Y axes, respectively. A positive Δ in $\text{Fe(II)}_{\text{AE}}$ concentration or negative Δ in Fe(III)_T concentration is taken to reflect net Fe(III)-reduction for that interval, whereas a negative Δ in $\text{Fe(II)}_{\text{AE}}$ or a positive Δ in Fe(III)_T concentration is taken to reflect net Fe(II)-oxidation for that interval, as indicated by the arrows at the top of both panels. The Pearson's correlation coefficient (r_p) and probability (p) are given in each panel.

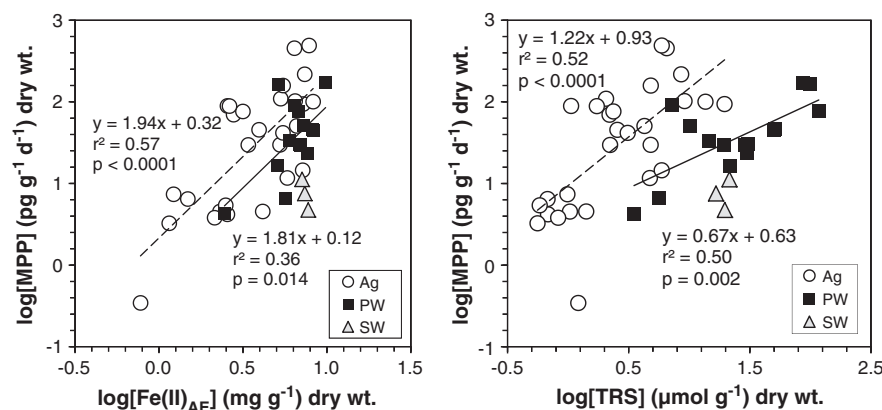


Fig. 5. X–Y plots of methylmercury production potential (MPP) rate data (LOG₁₀ transformed) versus A) acid extractable ferrous iron (Fe(II)_{AE}) (LOG₁₀ transformed), and B) total reduced sulfur (TRS) (LOG₁₀ transformed). The dashed and solid lines represent the least-squared regression for the agricultural (Ag) wetland and the permanent wetland (PW) data groupings, respectively. Data for the seasonal wetland (SW) grouping are plotted, but are not used in either regression. The coefficient of determination (r^2) and Type-II probability (p) of a non-zero slope are given along with each least-squares regression equation.

Bajita, 1995) may enhance the contribution of SR by replenishing sulfate through polysulfides (Rothenberg and Feng, 2012). This may also explain why C-flow estimates were generally higher for FeR in the agricultural wetlands during the growing season (Table 2), but TRS was more strongly correlated with k_{meth} (Fig. 3), than with the Fe metrics.

4. Conclusions

Through examination of sediment Fe, S, C, and Hg biogeochemistry, this study has demonstrated how conditions associated with agricultural wetland (rice cultivation) management can impact both the availability of Hg(II) for methylation and the activity of Hg(II)-methylating microbes. Overall, more MeHg was produced in surface sediment of agricultural wetlands than in non-agricultural wetlands. Sediment oxidation associated the drawdown of water on agricultural wetlands led to increased Hg(II)_R concentrations and a subsequent spike in MeHg production upon re-flooding during the post-harvest winter period, which was most pronounced in fields that were re-flooded to decay rice straw from the previous harvest. Evidence presented suggests that, compared to periods when agricultural soils were fully saturated, very high levels of both Hg(II)_R and MeHg can be preserved in drained and fully dried sediment. Upon re-flooding, some portion of MeHg flux from the sediment to the surface water may reflect the rapid release of MeHg formed during the preceding wet period. Microbial FeR appeared to dominate C-flow in agricultural wetlands during most of the year, although microbial SR was clearly also active. Periods of net oxidation or reduction, as reflected in temporal changes in bulk sediment Fe(III)_T and Fe(II)_{AE} pools, were strongly correlated with temporal changes in both Hg(II)_R and k_{meth} . While we could not definitively determine if SR or FeR dominated MeHg production, it is likely that both played a role to some degree. In agricultural wetlands, Fe(II)_{AE} concentration was equally good (if not slightly better) than was TRS concentration as a predictor of MeHg production potential rates.

Acknowledgments

The authors greatly acknowledge project funding from the California State Water Resources Control Board, under agreement number 06-232-555-0, through the San Jose State University Research Foundation; additional financial support from the USGS Toxics Program; and the contribution of sediment total mercury data in Fig. S2 by J. Holloway and M. Goldhaber (USGS, Denver, CO).

Appendix A. Supplementary data

Supplementary data to this article can be found online at <http://dx.doi.org/10.1016/j.scitotenv.2013.09.098>.

References

- Achnich C, Bak F, Conrad R. Competition for electron donors among nitrate reducers, ferric iron reducers, sulfate reducers, and methanogens in anoxic paddy soil. *Biol Fertil Soils* 1995;19:65–72.
- Ackerman JT, Eagles-Smith CA. Agricultural wetlands as potential hotspots for mercury bioaccumulation: experimental evidence using caged fish. *Environ Sci Technol* 2010;44:1451–7.
- Ackerman JT, Miles AK, Eagles-Smith CA. Invertebrate mercury bioaccumulation in permanent, seasonal, and flooded rice wetlands within California's Central Valley. *Sci Total Environ* 2010;408:666–71.
- Alpers CN, Hunerlach MP, May JT, Hothem RL. Mercury contamination from historical gold mining in California. Fact Sheet 2005–3014. US Geological Survey; 2005 6 p.
- Alpers CN, Fleck JA, Marvin-DiPasquale M, Stricker C, Stephenson M, Taylor HE. Mercury cycling in agricultural and managed wetlands, Yolo Bypass, California: Spatial and seasonal variations in water quality. *Sci Total Environ* 2013. [this issue].
- Bachand PAM, Bachand SM, Fleck JA, Anderson F, Windham-Myers L. Differentiating transpiration from evaporation in seasonal agricultural wetlands and the link to advective fluxes in the root zone. *Sci Total Environ* 2013. [this issue].
- Balci N, Shanks III WC, Mayer B, Mandernack KW. Oxygen and sulfur isotope systematics of sulfate produced by bacterial and abiotic oxidation of pyrite. *Geochim Cosmochim Acta* 2007;71:3796–811.
- Begg C, Kirk G, Mackenzie A, Neue HU. Root-induced iron oxidation and pH changes in the lowland rice rhizosphere. *New Phytol* 1994;128:469–77.
- Bodegom PMV, Stams AJM. Effects of alternative electron acceptors and temperature on methanogenesis in rice paddy soils. *Chemosphere* 1999;39:167–82.
- Bradley PM, Burns DA, Riva-Murray K, Brigham ME, Button DT, Chasar LC, et al. Spatial and seasonal variability of dissolved methylmercury in two stream basins in the eastern United States. *Environ Sci Technol* 2011;45:2048–55.
- Bridou R, Monperrus M, Gonzalez PR, Guyoneaud R, Amouroux D. Simultaneous determination of mercury methylation and demethylation capacities of various sulfate-reducing bacteria using species-specific isotopic tracers. *Environ Toxicol Chem* 2011;30:337–44.
- California Rice Commission. California Rice's Growing Region—A Circle of Life in Every Grain. Sacramento, California; 2011.
- Carmody RW, Plummer LN, Busenberg E, Copen TP. Methods for collection of dissolved sulfate and sulfide and analysis of their sulfur isotopic composition. Open-File Report 97-234. U.S. Geological Survey; 1998 91 p.
- Chanton JP, Whiting GJ, Blair NE, Lindau CW, Bollich PK. Methane emissions from rice: stable isotopes, diurnal variations, and CO₂ exchange. *Global Biogeochem Cycles* 1997;11:15–27.
- Compeau GC, Bartha R. Sulfate-reducing bacteria: principal methylators of mercury in anoxic estuarine sediment. *Appl Environ Microbiol* 1985;50:498–502.
- CVRWQCB. Amendments to the Water Quality Control Plan for the Sacramento River and San Joaquin River Basins for the Control of Methylmercury and Total Mercury in the Sacramento–San Joaquin River Delta Estuary; Resolution No. R5-2010-0043. Central Valley Regional Water Quality Control Board, Delta Mercury Control Program; 2011 36 p.
- Czech HA, Parsons KC. Agricultural wetlands and waterbirds: a review. *Waterbirds* 2002;25:56–65.
- Fang Y, Catron B, Zhang Y, Zhao L, Caruso JA, Hu Q. Distribution and in vitro availability of selenium in selenium-containing storage protein from selenium-enriched rice utilizing optimized extraction. *J Agric Food Chem* 2010;58:9731–8.

- Feng X, Li P, Qiu G, Wang S, Li G, Shang L, et al. Human exposure to methylmercury through rice intake in mercury mining areas, Guizhou province, China. *Environ Sci Technol* 2008;42:326–32.
- Finke N, Vandieken V, Jørgensen BB. Acetate, lactate, propionate, and isobutyrate as electron donors for iron and sulfate reduction in Arctic marine sediments, Svalbard. *FEMS Microbiol Ecol* 2007;59:10–22.
- Fleming EJ, Mack EE, Green PG, Nelson DC. Mercury methylation from unexpected sources: molybdate-inhibited freshwater sediments and an iron-reducing bacterium. *Appl Environ Microbiol* 2006;72:457–64.
- Giesemann A, Jager HJ, Norman AL, Krouse HR, Brand WA. On-line sulfur-isotope determination using an elemental analyzer coupled to a mass spectrometer. *Anal Chem* 1994;66:2816–9.
- Gilmour CC, Henry EA, Mitchell R. Sulfate stimulation of mercury methylation in freshwater sediments. *Environ Sci Technol* 1992;26:2281–7.
- Gilmour CC, Riedel GS, Ederington MC, Bell JT, Benoit JM, Gill GA, et al. Methylmercury concentrations and production rates across a trophic gradient in the northern Everglades. *Biogeochemistry* 1998;40:327–45.
- Hall BD, Aiken GR, Krabbenhoft DP, Marvin-DiPasquale M, Swarzenski CM. Wetlands as principal zones of methylmercury production in southern Louisiana and the Gulf of Mexico region. *Environ Pollut* 2008;154:124–34.
- Heim W, Coale K, Stephenson M, Choe K-Y, Gill G, Foe C. Spatial and habitat-based variations in total and methyl mercury concentrations in surficial sediments in the San Francisco Bay-Delta. *Environ Sci Technol* 2007;41:3501–7.
- Helsel DR. *Nondetects and Data Analysis: Statistics For Censored Environmental Data*. New York: John Wiley & Sons, Inc.; 2005.
- Horvat M, Nolde N, Fajon V, Jereb V, Logar M, Lojen S, et al. Total mercury, methylmercury and selenium in mercury polluted areas in the province Guizhou, China. *Sci Total Environ* 2003;304:231–56.
- Jørgensen BB. A comparison of methods for the quantification of bacterial sulfate reduction in coastal marine sediments. 1. Measurement with radiotracer techniques. *Geomicrobiol J* 1978;1:11–27.
- Kerin EJ, Gilmour CC, Roden E, Suzuki MT, Coates JD, Mason RP. Mercury methylation by dissimilatory iron-reducing bacteria. *Appl Environ Microbiol* 2006;72:7919–21.
- Kirk G. *The Biogeochemistry of Submerged Soils*. West Sussex, England: John Wiley and Sons; 2004.
- Kirk G, Bajita J. Root-induced iron oxidation, pH changes and zinc solubilization in the rhizosphere of lowland rice. *New Phytol* 1995;131:129–37.
- Kirk GJD, Du LV. Changes in rice root architecture, porosity, and oxygen and proton release under phosphorus deficiency. *New Phytol* 1997;135:191–200.
- Kirk GJ. Rice root properties for internal aeration and efficient nutrient acquisition in submerged soil. *New Phytol* 2003;159:185–94.
- Klüber HD, Conrad R. Effects of nitrate, nitrite, NO and N₂O on methanogenesis and other redox processes in anoxic rice field soil. *FEMS Microbiol Ecol* 1998;25:301–18.
- Lee RW, Kraus DW, Doeller JE. Oxidation of sulfide by *Spartina alterniflora* roots. *Limnol Oceanogr* 1999;44:1155–9.
- Liang F, Li Y, Zhang G, Tan M, Lin J, Liu W, et al. Total and speciated arsenic levels in rice from China. *Food Addit Contam Part A Chem Anal Control Expo Risk Assess* 2010;27:810–6.
- Liesack W, Schnell S, Revsbech NP. Microbiology of flooded rice paddies. *FEMS Microbiol Rev* 2000;24:625–45.
- Liu J, Cao C, Wong M, Zhang Z, Chai Y. Variations between rice cultivars in iron and manganese plaque on roots and the relation with plant cadmium uptake. *J Environ Sci (China)* 2010;22:1067–72.
- Lovley DR, Klug MJ. Model for the distribution of sulfate reduction and methanogenesis in freshwater sediments. *Geochim Cosmochim Acta* 1986;50:11–8.
- Lovley DR, Phillips EJP. Competitive mechanisms for inhibition of sulfate reduction and methane production in the zone of ferric iron reduction in sediments. *Appl Environ Microbiol* 1987a;53:2636–41.
- Lovley DR, Phillips EJP. Rapid assay for microbially reducible ferric iron in aquatic sediments. *Appl Environ Microbiol* 1987b;53:1536–40.
- Marvin-DiPasquale M, Agee J, Bouse R, Jaffe B. Microbial cycling of mercury in contaminated pelagic and wetland sediments of San Pablo Bay, California. *Environ Geol* 2003a;43:260–7.
- Marvin-DiPasquale M, Agee J, McGowan C, Oremland RS, Thomas M, Krabbenhoft D, et al. Methyl-mercury degradation pathways: a comparison among three mercury-impacted ecosystems. *Environ Sci Technol* 2000;34:4908–16.
- Marvin-DiPasquale M, Agee JL. Microbial mercury cycling in sediments of the San Francisco Bay-Delta. *Estuaries* 2003;26:1517–28.
- Marvin-DiPasquale M, Agee JL, Kakouros E, Kieu LH, Fleck JA, Alpers CN. The effects of sediment and mercury mobilization in the South Yuba River and Humbug Creek confluence area, Nevada County, California: concentrations, speciation and environmental fate—Part 2: Laboratory experiments. Open-File Report 2010–1325B. U.S. Geological Survey; 2011 53 p.
- Marvin-DiPasquale M, Alpers CN, Fleck JA. Mercury, methylmercury, and other constituents in sediment and water from seasonal and permanent wetlands in the Cache Creek Settling Basin and Yolo Bypass, Yolo County, California, 2005–06. Open File Report 2009-1182. U.S. Geological Survey; 2009a 69 p.
- Marvin-DiPasquale M, Lutz MA, Brigham ME, Krabbenhoft DP, Aiken GR, Orem WH, et al. Mercury cycling in stream ecosystems. 2. Benthic methylmercury production and bed sediment-pore water partitioning. *Environ Sci Technol* 2009b;43:2726–32.
- Marvin-DiPasquale M, Lutz MA, Brigham ME, Krabbenhoft DP, Aiken GR, Orem WH, et al. Mercury cycling in stream ecosystems: 2. Benthic methylmercury production and bed sediment-pore water partitioning. *Environ Sci Technol* 2009c;43:2726–32.
- Marvin-DiPasquale MC, Boynton WR, Capone DG. Benthic sulfate reduction along the Chesapeake Bay central channel. II. Temporal controls. *Mar Ecol Prog Ser* 2003b;260:55–70.
- Marvin-DiPasquale MC, Lutz MA, Krabbenhoft DP, Aiken GR, Orem WH, Hall BD, et al. Total mercury, methylmercury, methylmercury production potential, and ancillary streambed-sediment and pore-water data for selected streams in Oregon, Wisconsin, and Florida, 2003–04. Data Series 375. U.S. Geological Survey; 2008 25 p.
- Matthes WJ, Sholar CJ, George JR. Quality-assurance plan for the analysis of fluvial sediment by laboratories of the U.S. Geological Survey. Open-File Report 91–467. U.S. Geological Survey; 1992 37 p.
- Meng B, Feng X, Qiu G, Cai Y, Wang D, Li P, et al. Distribution patterns of inorganic mercury and methylmercury in tissues of rice (*Oryza sativa* L.) plants and possible bioaccumulation pathways. *J Agric Food Chem* 2010;58:4951–8.
- Mitchell CP, Branfireun BA, Kolka RK. Methylmercury dynamics at the upland-peatland interface: topographic and hydrogeochemical controls. *Water Resour Res* 2009;45. <http://dx.doi.org/10.1029/2008WR006832>. [W02406].
- National Research Council. *Wetlands: characteristics and boundaries*. Washington, DC: National Academy Press; 1995.
- Reichardt W, Mascarina G, Padre B, Doll J. Microbial communities of continuously cropped, irrigated rice fields. *Appl Environ Microbiol* 1997;63:233–8.
- Roden EE, Lovley DR. Evaluation of ⁵⁵Fe as a tracer of Fe(III) reduction in aquatic sediments. *Geomicrobiol J* 1993;11:49–56.
- Roden EE, Tuttle JH. Inorganic sulfur turnover in oligohaline estuarine sediments. *Biogeochemical* 1993;22:81–105.
- Roden EE, Wetzel RG. Kinetics of microbial Fe(III) oxide reduction in freshwater wetland sediments. *Limnol Oceanogr* 2002;47:198–211.
- Roden EE, Zachara JM. Microbial reduction of crystalline iron(III) oxides: influence of oxide surface area and potential for cell growth. *Environ Sci Technol* 1996;30:1618–28.
- Rothenberg SE, Feng X. Mercury cycling in a flooded rice paddy. *J Geophys Res* 2012;117.
- Rothenberg SE, Feng X, Dong B, Shang L, Yin R, Yuan X. Characterization of mercury species in brown and white rice (*Oryza sativa* L.) grown in water-saving paddies. *Environ Pollut* 2011;159:1283–9.
- Rothenberg SE, Feng X, Zhou W, Tu M, Jin B, You J. Environment and genotype controls on mercury accumulation in rice (*Oryza sativa* L.) cultivated along a contamination gradient in Guizhou, China. *Sci Total Environ* 2012;426:272–80.
- Roulet M, Guimaraes JRD, Lucotte M. Methylmercury production and accumulation in sediments and soils of an amazonian floodplain—effect of seasonal inundation. *Water Air Soil Pollut* 2001;128:41–60.
- Sellers P, Kelly CA, Rudd JWM, MacHutchison AR. Photodegradation of methylmercury in lakes. *Nature* 1996;380:694–6.
- Sharp Z. *Principles of stable isotope geochemistry*. New Jersey: Pearson-Prentice Hall; 2007.
- Shi JB, Liang LN, Jiang GB. Simultaneous determination of methylmercury and ethylmercury in rice by capillary gas chromatography coupled on-line with atomic fluorescence spectrometry. *J AOAC Int* 2005;88:665–9.
- USDA. *Rice Yearbook 2012. Table 6—State and U.S. rice production by class*. U.S. Dept. of Agriculture; 2012.
- vanderGon HACD, Neue HU. Oxidation of methane in the rhizosphere of rice plants. *Biol Fertil Soils* 1996;22:359–66.
- Windham-Myers L, Ackerman JT, Fleck JA, Marvin-DiPasquale M, Stricker CA, Bachand P, Eagles-Smith CA, Feliz D, Gill G, Stephenson M, Alpers CN. Mercury cycling in agricultural and managed wetlands: A synthesis of observations from an integrated field study of methylmercury production, hydrologic export, and bioaccumulation. *Sci Total Environ* 2013. [in this issue-a].
- Windham-Myers L, Marvin-DiPasquale M, Kakouros E, Agee JL, Kieu LH, Stricker C, Fleck JA, Alpers CN, Ackerman JT. Mercury cycling in agricultural and managed wetlands, Yolo Bypass, California: Seasonal influences of vegetation on mercury methylation, storage, and transport. *Sci Total Environ* 2013. [in this issue-b].
- Windham-Myers L, Marvin-DiPasquale M, Krabbenhoft DP, Agee JL, Cox MH, Heredia-Middleton P, et al. Experimental removal of wetland emergent vegetation leads to decreased methylmercury production in surface sediment. *J Geophys Res Biogeosci* 2009;114. <http://dx.doi.org/10.1029/2008JG000815>. (G00C05).
- Windham-Myers L, Marvin-DiPasquale M, Stricker C, Agee JL, Kieu L, Kakouros E. Mercury cycling in agricultural and managed wetlands, Yolo Bypass, California: Experimental evidence of vegetation-driven changes in sediment biogeochemistry and methylmercury. *Sci Total Environ* 2013. [in this issue-c].
- Yun H, Zhang L, Li X, Zhao Y, Wu Y. Determination of inorganic arsenic in rice by liquid chromatography-atomic fluorescence spectrometry. *Wei Sheng Yan Jiu* 2010;39:316–20.
- Zhang H, Feng X, Larssen T, Shang L, Li P. Bioaccumulation of methylmercury versus inorganic mercury in rice (*Oryza sativa* L.) grain. *Environ Sci Technol* 2010;44:4499–504.